
ELECTRICAL AND MAGNETIC
PROPERTIES

Magneto-Optical Detection of the Intrinsic Ferromagnetism and Phase Separation in Diluted Magnetic Semiconductors

E. A. Gan'shina^a, L. L. Golik^b, Z. E. Kun'kova^{b, *}, G. S. Zykova^a,
A. I. Rukovishnikov^b, and Yu. V. Markin^b

^a*Lomonosov Moscow State University, Moscow, 119991 Russia*

^b*Kotel'nikov Institute of Radioengineering and Electronics, Russian Academy of Sciences, Fryazino Branch, Fryazino, Moscow oblast, 141190 Russia*

**e-mail: z.kunkova@gmail.com*

Received September 16, 2019; revised October 8, 2019; accepted October 10, 2019

Abstract—Spectral and temperature dependences of the magneto-optical transversal Kerr effect (TKE) of GaMnAs layers prepared by different methods are reported in this work. The GaMnAs layers prepared by pulsed laser sputtering at 300°C demonstrate a ferromagnetic behavior below 80 K, which is due to the presence of local ferromagnetic (Ga,Mn)As areas in the paramagnetic matrix. The Ga(In)MnAs layers prepared by ion implantation and subsequent pulsed laser annealing were found to exhibit a high TKE response at low temperatures. The presence of the characteristic band in the TKE spectrum in the range of transitions near the *L* point of the band structure of Ga(In)As confirms the intrinsic ferromagnetism. The temperature dependences of TKE measured for different spectrum ranges demonstrate nonmonotonic behavior, which indicates the magnetic inhomogeneity of the layers. The peculiarities of the magneto-optical spectra of GaMnAs, which were not observed previously, were explained by taking the magnetic and phase inhomogeneity of the layers into account. The sensitivity of TKE to the phase inhomogeneity of the Ga(In)MnAs layers and the efficiency of TKE in studying the electron spectrum and magnetic structure of diluted magnetic superconductors are demonstrated.

Keywords: diluted magnetic semiconductors, GaMnAs, magneto-optical spectroscopy, transversal Kerr effect

DOI: 10.1134/S0031918X20030047

INTRODUCTION

Diluted magnetic semiconductors (DMSs) are promising materials for spintronics; however, to use their functional possibilities, the Curie temperature of the materials should be substantially above the room temperature. The room-temperature ferromagnetism has been found for a wide range of materials in the last two decades. However, a number of sources of nonintrinsic ferromagnetic behavior of DMSs were found; these are magnetic impurities, instrumental artifacts, and secondary magnetic phases [1]. Because of this, reports on high-temperature DMSs should include reliable confirmation of the intrinsic ferromagnetic nature. To obtain such confirmation, modern methods of structural and magnetic diagnostics, such as transmission electron microscopy, X-ray diffraction, X-ray magnetic circular dichroism, etc. should be used along with traditional laboratory methods (magnetometry, electrical and magnetotransport measurements). However, these complex and expensive methods are not always available.

It is known that the intrinsic ferromagnetism of DMSs can be seen in peculiarities observed in mag-

neto-optical spectra, whose energy position is determined by the band structure of the parent semiconductor. This makes magneto-optical spectroscopy an efficient method for the diagnostics and investigation of DMSs, which allows one to record the appearance of ferromagnetism, to find the presence of secondary magnetic phases, and to obtain detailed information about the electronic spectrum of DMSs [2–4].

The topical points of the physics of DMSs include the interplay between ferromagnetism and localization of carriers and the evolution of ferromagnetism in them. The coexistence of strong effects of exchange coupling between carriers and localized spins with the localization phenomena in disordered systems is one of the characteristic peculiarities of DMSs. The problem of the mutual effect of ferromagnetism and localization is particularly relevant for Ga(In)MnAs compounds. In these compounds, the carriers that participated in the ferromagnetic exchange are simultaneously subjected to localization [5–9]. Understanding of the interplay between the ferromagnetism and localization is still at an early stage. This is related to both insufficient development of the theory of metal–insulator transition (MIT) for DMSs and strong dependence of

Table 1. Fluence of Mn ions and characteristics of $\text{Ga}_{1-x}\text{Mn}_x\text{As}$ and $\text{In}_{1-x}\text{Mn}_x\text{As}$ layers

$\text{Ga}_{1-x}\text{Mn}_x\text{As}$, no.	W , cm^{-2}	x	T_C , K	$\text{In}_{1-x}\text{Mn}_x\text{As}$, no.	W , cm^{-2}	x	T_C , K
1-G	1×10^{15}	0.0066	(7.5)	1-I	4×10^{15}	0.019	14
2-G	1.5×10^{15}	0.0087	17	2-I	8×10^{15}	0.042	40
3-G	2×10^{15}	0.012	31	3-I	1.6×10^{16}	0.069	77
4-G	8×10^{15}	0.018	60	4-I	2.8×10^{16}	0.105	82
5-G	1×10^{16}	~ 0.033	60				

the localization and magnetic properties on the concentration of donor defects (Mn ions present in interstices and antistructural As ions), which are difficult to control. The presence of randomly distributed acceptors (Mn ions occupied lattice sites) leads to the substantial disorder, fluctuations of local carrier density, and electronic phase separation in GaMnAs [9]. The latter phenomenon can be accompanied by the metal–insulator transition and the formation of nano-sized metallic ferromagnetic areas in the paramagnetic matrix. The coexistence of different magnetic phases was observed experimentally in GaMnAs layers prepared by low-temperature molecular-beam epitaxy (LT-MBE) [7, 10, 11] and ion implantation followed by pulsed laser annealing (II-PLA) [12, 13]. The magneto-optical spectroscopy is sensitive not only to the long-range magnetic order but also to the appearance of short-range order; the presence of magnetic inhomogeneities can be seen in the appearance of additional peculiarities in spectra and temperature dependences of MO signal.

The kinds of stacking faults and point defects and, therefore, the concentration of free carriers, the position of the Fermi level, and the character of phase inhomogeneities all depend on the growth technology. The majority of MO investigations were performed for GaMnAs layers prepared by LT-MBE technology [3 and references in 16]. DMSs formed by II-PLA are also of interest since defects related to the interstitial Mn and antistructural As ions are almost absent in these DMSs.

We used MO spectroscopy to study the properties of the Ga(In)MnAs layers prepared by pulsed laser sputtering (PLS) and II-PLA [4, 14–17]. In the present work, we report experimental data that demonstrate the efficiency of MO spectroscopy for the detection of secondary magnetic phases, confirmation of the intrinsic ferromagnetism, and study of peculiarities of electronic spectrum of DMSs. The sensitivity of MO spectroscopy to the electronic phase separation in DMSs is demonstrated.

EXPERIMENTAL

A number of the GaMnAs samples were prepared by pulsed laser sputtering in the Scientific Research

Physicotechnical Institute at the National Research Lobachevskii State University [18]. The amount of Mn in the layers was controlled by the relationship of times of sputtering of Mn and GaAs targets, $Y_{\text{Mn}} = t_{\text{Mn}}/(t_{\text{Mn}} + t_{\text{GaAs}})$. We report below the results of the investigation of GaMnAs/*i*-GaAs(001) (samples 1–4) formed at $Y_{\text{Mn}} = 0.13$ and 0.23 and substrate temperatures $T_g = 300, 330,$ and 350°C . The GaMnAs layer thickness in samples 1–3 is 130 nm; the layer thickness in sample 4 is 100 nm.

The $\text{Ga}_{1-x}\text{Mn}_x\text{As}$ and $\text{In}_{1-x}\text{Mn}_x\text{As}$ layers prepared by the II-PLA method in the Ion Beam Center at the Helmholtz-Zentrum Dresden-Rossendorf were also studied. Data on the preparation of the samples are available in [12, 19]. Data on the Mn distribution across the layer thickness, TEM data, and the results of electrical measurements and magnetometry of the $\text{Ga}_{1-x}\text{Mn}_x\text{As}$ layers are given in [13]. Information about the preparation of the $\text{In}_{1-x}\text{Mn}_x\text{As}$ layers and magnetometry and X-ray diffraction data are given in [20]. The effective thickness of the layers formed by II-PLA is 80 nm. Table 1 shows the fluence of Mn ions (W), Mn concentration (x), and Curie temperature of the layers (T_C).

The magneto-optical properties of the DMS layers were studied using the transversal Kerr effect (TKE), which consists in measuring the intensity of *p* polarized light reflected by a sample upon magnetization in the magnetic field applied in parallel to the sample surface and perpendicular to the plane of light incidence. The TKE value is $\delta = [I(H) - I(-H)]/2I(0)$, where $I(H)$ and $I(0)$ is the intensity of reflected light in the presence and absence of magnetic field, respectively; it was measured by dynamic method upon magnetic field modulation.

The TKE spectra $\delta(E)$ were measured in the energy range $E = 0.5\text{--}4.0$ eV in magnetic fields up to 3 kOe. The temperature range of the investigations is $T = 15\text{--}295$ K; the instrument sensitivity to changes in the light intensity is $\sim 10^{-5}$. To analyze the magnetic structure of the layers, temperature $\delta(T)$ and field $\delta(H)$ dependences of TKE were measured in different ranges of the spectrum.

RESULTS AND DISCUSSION

Figure 1 shows the TKE spectra $\delta(E)$ for the GaMnAs layers (samples 1–4) formed by PLS. Insets show the temperature dependences $\delta(T)$, measured at fixed energies. The given curves demonstrate changes in the character of TKE spectra, which are observed with changing growth conditions. Samples 1–3 exhibit a sufficiently large signal even at room temperature (T_{room}). As the temperature decreases, the signal increases and spectral peculiarities become clearly pronounced. The TKE spectra of sample 1 formed at the maximum parameters $Y_{\text{Mn}} = 0.23$ and $T_{\text{g}} = 350^\circ\text{C}$ (Fig. 1a) are typical for the GaMnAs layers containing “bulk” inclusions of the MnAs ferromagnet ($T_{\text{C}} = 318$ K). Peculiarities corresponding to energies of 1.8, 2.5, and 3.5 eV are due to the optical transitions in MnAs [21]. The curve given in the inset is analogous to the dependence $\delta(T)$ of the reference MnAs sample. As the temperature T_{g} decreases to 300°C , the resonance structure in the range $E = 0.5$ – 2.0 eV becomes dominant in the spectrum of sample 2 (Fig. 1b). We showed that the structure is due to the excitation of surface plasmons in MnAs nanoclusters [4, 14]. The shape of the curve $\delta(T)$ for sample 2 is determined mainly by the contribution of MnAs inclusions; in the low-temperature range, a weak increase in the effect is observed, which is related to the contribution of doped matrix.

Figure 1c shows the TKE spectra of sample 3 ($Y_{\text{Mn}} = 0.13$ and $T_{\text{g}} = 330^\circ\text{C}$) measured at three different temperatures. The comparison of the spectra with those given in Figs. 1a, 1b shows that the spectra of sample 3, which were measured at $T = 295$ and 120 K, contain contributions of the transitions in “bulk” MnAs and plasmons in the MnAs nanoclusters (the peculiarity in a range of 1.0–1.5 eV). The region corresponding to the marked increase in the dependence $\delta(T)$ below 80 K indicates the presence of a low-temperature magnetic phase. Since, at low temperatures, the signal from “bulk” MnAs and plasmon signal change slightly, the spectral contribution of the low-temperature phase can be separated by subtracting the spectrum measured at $T = 120$ K from that measured at $T = 30$ K. The separated contribution, $\delta(E) = \delta(E)_{30\text{ K}} - \delta(E)_{120\text{ K}}$, is given in Fig. 1c (curve without symbols).

The TKE signal of sample 4 ($Y_{\text{Mn}} = 0.13$, $T_{\text{g}} = 300^\circ\text{C}$) at room temperature (T_{room}) is close to noise level and is related to the presence of MnAs “traces.” The inset in Fig. 1d shows that, upon cooling to 85 K, the signal increases and remains insignificant but abruptly increases below 80 K. The temperature and magnetic-field dependences of TKE indicate the presence of a ferromagnetic phase with $T_{\text{C}} \approx 80$ K in sample 4. Figure 1d shows the TKE spectra of sample 4 at $T = 80$ and 25 K; dashed lines indicate the energies of transitions E_0 , $E_0 + \Delta_0$ and E_1 , $E_1 + \Delta_1$ at the Γ and L critical points of the Brillouin zone of GaAs. At $T =$

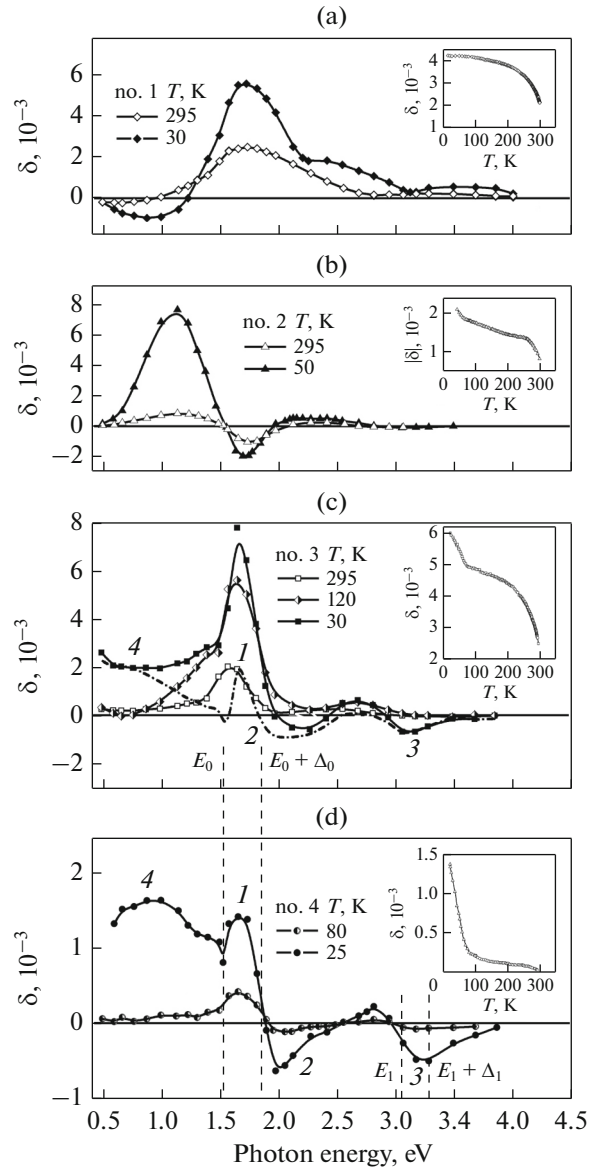


Fig. 1. TKE spectra of samples 1–4 measured at T_{room} and low temperatures. Dashed lines correspond to the energies of the transitions E_0 , $E_0 + \Delta_0$ and E_1 , $E_1 + \Delta_1$ at the Γ and L points of GaAs at $T = 22$ K [22]. Curve without symbols in Fig. 1c corresponds to $\delta(E) = \delta(E)_{30\text{ K}} - \delta(E)_{120\text{ K}}$. Insets show the dependences $\delta(T)$ measured for samples 1, 2, 3, and 4 at energies E of 1.97, 1.73, 1.65, and 1.73 eV, respectively.

25 K, the $\delta(E)$ spectrum exhibit four clear bands designated by digits 1–4. Bands 1 and 2 are shifted to the high-energy range ($E_{\text{max}1} = 1.65$ eV; $E_{\text{max}2} = 2.0$ eV) with respect to the transitions E_0 and $E_0 + \Delta_0$ (blue shift). Band 3 ($E_{\text{max}3} \approx 3.2$ eV) is localized in the range of transitions E_1 and $E_1 + \Delta_1$. In the impurity absorption range of GaAs, band 4 is observed. Bands 1–4 also are present in the difference curve at close energies (Fig. 1c). Changes in the electronic spectrum of

the parent semiconductor, which are caused by high concentrations of introduced transition metal, weakly affect the optical transitions in the vicinity of the point L apart from the centre of Brillouin zone. Because of this, the presence of a band in the magneto-optical spectra in the range of the transitions E_1 and $E_1 + \Delta_1$ indicates the intrinsic magnetism of DMSs. Band 3 is clearly defined in the TKE spectrum of sample 4; therefore, the ferromagnetism is due to the (Ga,Mn)As phase. The MnAs content in sample 4 is insignificant and does not affect its properties (is not recorded by magnetometry).

It follows from data given in Fig. 1c that (Ga,Mn)As DMS is also present in sample 3, along with MnAs in the form of bulk and nano-sized inclusions.

The magnetic (at T_{room}), electrical, and magnetotransport measurements were performed using samples belonging to the same growth series [17]. The magnetometry indicated the presence of a significant amount of the MnAs phase in sample 1; its content in sample 3 is substantially lower. No magnetization was recorded in performing measurements for samples 2 and 4. Measurements performed on a HR Bruker D8 Discover X-ray diffractometer indicated the presence of Mn only in sample 1; therefore, the sensitivity of the device is insufficient to detect MnAs in the other samples. At the same time, the application of the MO method allowed us to find MnAs in all samples and the presence of (Ga,Mn)As DMS in samples 4 and 3.

Samples 2 and 4 are characterized by high electrical resistivity, which increases rapidly below 80 K. The ferromagnetism of sample 4 characterized by the rather high Curie temperature $T_C \approx 80$ K does not agree with the high electrical resistivity and low concentration of holes ($p \sim 2 \times 10^{19} \text{ cm}^{-3}$ at $T = 295$ K). This discrepancy is eliminated in the case of chemical phase separation [9], when the substantially inhomogeneous Mn distribution leads to the appearance of ferromagnetic nanoclusters in the paramagnetic matrix, which are characterized by increased concentrations of Mn and holes. For such an inhomogeneous sample, measurements of transport properties probe the paramagnetic matrix, whereas TKE probes the (Ga,Mn)As ferromagnetic areas. The blue shift of bands 1 and 2 in the TKE spectrum of sample 4 can be caused by the shift of the Fermi level deep down the valence band and size quantization in ferromagnetic nanoclusters. The anomalous Hall effect (AHE) is observed at $T < 60$ K for sample 3 (characterized by the low electrical resistivity), in which (Ga,Mn)As DMS is present. AHE indicates the low-temperature ferromagnetism of the matrix in sample 3 and is likely to be related to the overlap of the ferromagnetic (Ga,Mn)As areas and the formation of ways for the current flowing.

Figure 2 shows spectral and temperature dependences of TKE of the $\text{Ga}_{1-x}\text{Mn}_x\text{As}$ (1-G-5-G) sam-

ples prepared by II-PLA. The TKE signal is not recorded at room temperature; therefore, MnAs is absent in the samples under study. The magnetic field dependences of TKE (not shown here) indicate the ferromagnetism of samples 2-G-5-G at low temperatures (at the measurement temperatures, sample 1-G remains paramagnetic). The TKE spectra of all samples at $T = 17$ K (Fig. 2a) demonstrate the strong MO response. In the range of transitions $E_1, E_1 + \Delta_1$, the characteristic band is well defined; its enlarged image is shown in inset in Fig. 2a. The spectra of samples 1-G-4-G in the range $E \approx 1.1-2.25$ eV exhibit a negative polarity band with two local minima in the range of transitions E_0 and $E_0 + \Delta_0$. As x increases, these peculiarities increase, and their slight blue shift is observed. The negative band becomes markedly more intense in the spectrum of sample 5-G; single minimum in the band is observed near 1.6 eV. The MO spectra shown in Fig. 2a differ from those of the $\text{Ga}_{1-x}\text{Mn}_x\text{As}$ samples prepared by LT-MBE [15]. The peculiarity of the $\text{Ga}_{1-x}\text{Mn}_x\text{As}$ samples prepared by II-PLA is the Gaussian Mn distribution across the thickness and the electronic phase separation found at the Mn concentrations $x < 0.014$ [13]. Taking this into account, we relate the wide negative band in the TKE spectra with the superposition of contributions from regions characterized by the different concentrations of Mn and/or holes [16]. The changed shape of the band in the 5-G sample spectrum may result from the opposite concentration shifts of the contributions of these regions.

The magnetic (phase) inhomogeneity of samples can be probed by measuring the temperature dependences of TKE. For homogeneous samples, the curves $\delta(T)$ indicate the monotonic increase in the magnetization upon cooling; the dependences reduced to the maximum value $\delta(T)/\delta_{\text{max}}$ are independent of the photon energy. In inhomogeneous samples, the regions differing in characteristics can make contributions of opposite polarity; in the case of the comparable contributions, the resulting signal may be decreased. The sufficiently high measuring field can order nano-sized ferromagnetic regions arising at a temperature slightly higher than the Curie temperature T_C , blur the dependences $\delta(T)$, and increase the effective T_C value, which is determined by the extrapolation of the abrupt-drop portion in the curve $\delta(T)$. To decrease this effect, the dependences $\delta(T)$ were measured in high and low magnetic fields. The TKE signal decreases as the field H decreases; to find the qualitative changes in the temperature curves, we compare the reduced dependences $\delta(T)/\delta_{\text{max}}$. Figures 2b-2e show several examples of the temperature dependences for samples 3-G-5-G, which were measured near extremes of the negative band ($E = 1.54-1.73$ eV) and in the range of low signals ($E = 2.41$ eV). For comparison, Fig. 2d shows also the dependences $\delta(T)/\delta_{\text{max}}$ for the $\text{Ga}_{1-x}\text{Mn}_x\text{As}$ ($x = 0.06$) sample (curves 3 and 4); the sample has been prepared by LT-MBE and is char-

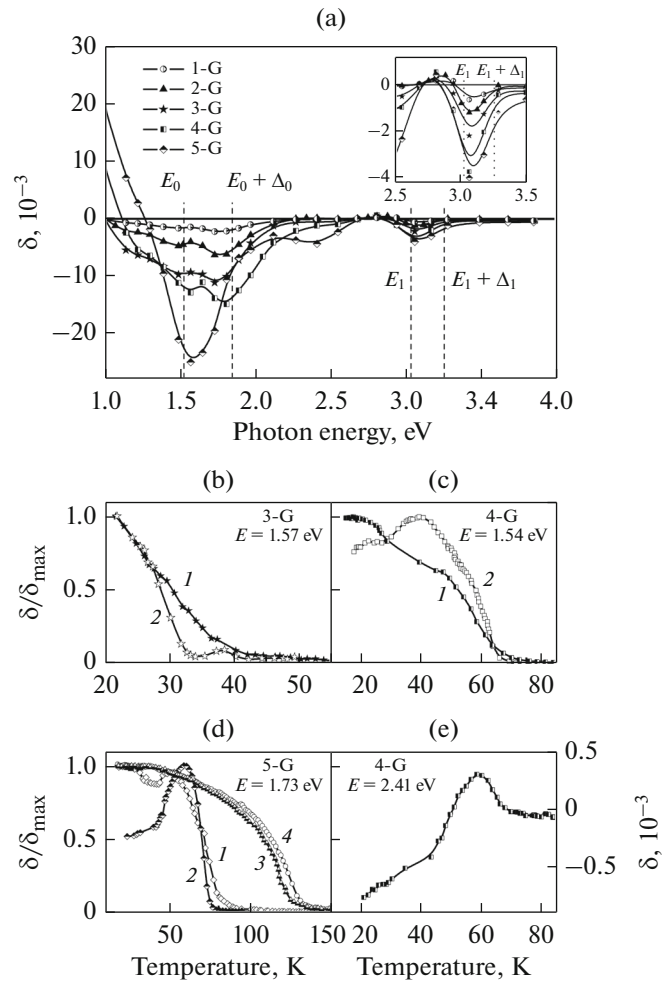


Fig. 2. (a) TKE spectra of samples 1-G–5-G measured at $T = 17$ K. Dashed lines correspond to the energies of the transitions at the Γ and L points of GaAs; inset shows the enlarged image of the band in the range of the transitions at the L point of GaAs. (b–d) Dependences $\delta(T)/\delta_{\max}$ for samples 3-G–5-G for two different amplitudes of magnetic field H , Oe: (b) 1–1300, 2–100; (c) 1–2500, 2–95; and (d) 1–1600, 2–95. For reference sample (Ga,Mn)As prepared by LT-MLE, $H = 2500$ Oe; curves 3 and 4 measured at $E = 1.65$ and $E = 3.06$ eV. (e) Dependence $\delta(T)$ for sample 4-G; $H = 150$ Oe.

acterized by the metallic conductivity and $T_C \approx 130$ K. Curves 3 and 4 measured for two energies in the field $H = 2500$ Oe differ slightly and demonstrate the monotonic increase upon cooling, which is typical for homogeneous samples.

Figure 2b illustrates the change in the dependence $\delta(T)/\delta_{\max}$ for sample 3-G ($x = 0.012$) as the field decreases from 1300 to 100 Oe. The estimation of T_C in the field of 1300 Oe (curve 1) gives the value $T_C \approx 40$ K. Curve 2 measured in the weak field exhibits contributions from regions with $T_C \approx 32$ K (the main contribution with T_C close to that determined by magnetometry) and with $T_C \approx 42$ K (weak contribution), which confirm the magnetic inhomogeneity of the sample. Figures 2c and d show the dependences $\delta(T)/\delta_{\max}$ for samples 4-G and 5-G with the Mn concentrations exceeding the value $x = 0.014$, which is the boundary for the formation of “global” ferromagnetism, respec-

tively [13]. The substantial difference in the behavior of curves 1 and 2 is observed. They exhibit peculiarities at low temperatures, which are clearer in measuring in the low field, when the increase in TKE upon cooling changes to the decrease.

In the range of measurements of curves 1 and 2, the TKE signal polarity is negative (Fig. 2a), and the decrease in the signal indicates the presence of positive contribution and its increase upon cooling. The presence of positive-polarity contribution in the spectrum was found in measurements in the range of weak signals. Figure 2d shows the dependence $\delta(T)$ for sample 4-G ($E = 2.41$ eV), which demonstrates the appearance of positive signal at $T \approx 70$ K and the change of the polarity below 50 K. The relative decrease in the TKE signal with decreasing temperature depends on the measuring range; the positive contribution from TKE cannot be explained only by the monotonically descending “tail” of the impurity band, which was observed in [3].

Metallic ferromagnetic inclusions with higher T_C and regions with lower hole concentration and T_C , in whose spectra the “positive” band is present near the transitions $E_0 + \Delta_0$, can also be the sources of signals having the positive polarity.

The boundary value $x = 0.014$, at which the “global” ferromagnetism without a superparamagnetic phase appears in the II-ILA $\text{Ga}_{1-x}\text{Mn}_x\text{As}$ layers, was determined in [13] from the absence of the manifestation of the blocking of superparamagnetic clusters in the thermo-remnant magnetization curves. At the same time, the nonmonotonic behavior of the dependences $\delta(T)$ indicates magnetic inhomogeneity in samples 4-G and 5-G, whose Mn concentration exceeds the boundary value x . The cause for the difference may be the rise of ferromagnetic inclusions with increasing the Mn concentration and the possibility of magneto-optical observation of particles whose size exceeds that of superparamagnetic clusters.

We also studied the MO properties of the $\text{In}_{1-x}\text{Mn}_x\text{As}$ samples, 1-I–4-I, prepared by II-PLA method. The high TKE signals are observed near the absorption edge. The intrinsic ferromagnetism is confirmed by the presence of extremes in the MO spectra in the range of transitions E_1 and $E_1 + \Delta_1$ in InAs. The nonmonotonic behavior of the dependences $\delta(T)$ and $\delta(H)$ upon cooling exhibits the magnetic inhomogeneity of the $\text{In}_{1-x}\text{Mn}_x\text{As}$ samples at the higher Mn concentrations as compared to those ($x \leq 0.012$) determined in [13]. The results of these studies will be presented elsewhere.

CONCLUSIONS

The application of magneto-optical spectroscopy allowed us to detect the intrinsic ferromagnetism of the GaMnAs samples with $T_C \leq 80$ K, which were prepared by PLS at low values of the growth parameters. Local ferromagnetic regions (Ga,Mn)As present in the weakly doped paramagnetic matrix are the source of the TKE signal. The peculiarity of the TKE spectrum (the blue shift of bands) can be caused by the shift of the Fermi level to deep down the valence band and the size quantization in ferromagnetic nano-sized regions. The increase in the growth parameters leads to the coexistence of cubic (Ga,Mn)As and hexagonal MnAs nano-sized regions and, after that, to the formation of MnAs particles retaining the properties of the bulk material.

For the Ga(In)MnAs layers prepared by the II-PLA method, the high TKE signal is recorded at low temperatures. Secondary magnetic phases are absent in the layers. The presence, in the TKE spectra, of the characteristic band in the range of transitions at the L point of the band structure of Ga(In)As confirms the intrinsic ferromagnetism of the layers. The nonmonotonic behavior of the temperature dependences of TKE indicates the magnetic inhomogeneity of the

layers. The peculiarities, which were not previously observed in magneto-optical spectra of GaMnAs, are explained by the presence of nano-sized regions in the semiconducting matrix, which are characterized by the higher carrier concentration and Curie temperature and the shift of the Fermi level deep down the valence band. The reported results demonstrate the sensitivity of TKE to the phase inhomogeneity of Ga(In)MnAs and the efficiency of TKE in studying the electronic spectrum and magnetic structure of DMSs and also in characterizing samples.

ACKNOWLEDGMENTS

We thank Dr. S. Zhou, Dr. Yu.A. Danilov, and Dr. B.N. Zvonkov for the DMSs samples provided.

FUNDING

The study was performed within the framework of a state task.

REFERENCES

1. L. M. C. Pereira, “Experimentally evaluating the origin of dilute magnetism in nanomaterials,” *J. Phys. D: Appl. Phys.* **50**, No. 39, 393002 (26pp) (2017).
2. K. Ando, “Magneto-optics of diluted magnetic semiconductors: New materials and applications, in *Magneto-Optics*, Ed. by S. Sugano and N. Kojima (Springer, Berlin, 2000), vol. 128, pp. 211–241.
3. K. Ando, H. Saito, K. C. Agarwal, M. C. Debnath, and V. Zayets, “Origin of the anomalous magnetic circular dichroism spectral shape in ferromagnetic $\text{Ga}_{1-x}\text{Mn}_x\text{As}$: Impurity bands inside the band gap,” *Phys. Rev. Lett.* **100**, 067204 (2008).
4. E. A. Gan'shina, L. L. Golik, V. I. Kovalev, Z. E. Kun'kova, A. G. Temiryazev, Yu. A. Danilov, O. V. Vikhrova, B. N. Zvonkov, A. D. Rubacheva, P. N. Tcherbak, A. N. Vinogradov, and O. M. Zhigalina, “Resonant enhancement of the transversal Kerr effect in the InMnAs layers,” *J. Phys.: Cond. Mater.* **22**, 396002 (2010).
5. T. Dietl, H. Ohno, F. Matsukura, J. Cibert, and D. Ferrand, “Zener model description of ferromagnetism in zinc-blende magnetic semiconductors,” *Science* **287**, 1019–1022 (2000).
6. T. Dietl, “Interplay between carrier localization and magnetism in diluted magnetic and ferromagnetic semiconductors,” *J. Phys. Soc. Jpn.* **77**, 031005 (2008).
7. M. Sawicki, D. Chiba, A. Korbecka, Y. Nishitani, J. A. Majewski, F. Matsukura, T. Dietl, and H. Ohno, “Experimental probing of the interplay between ferromagnetism and localization in (Ga,Mn)As,” *Nat. Phys.* **6**, 22–25 (2010).
8. A. X. Gray, J. Minar, S. Ueda, P. R. Stone, Y. Yamashita, J. Fujii, J. Braun, L. Plucinski, C. M. Schneider, G. Panaccione, H. Ebert, O. D. Dubon, K. Kobayashi, and C. S. Fadley, “Bulk electronic structure of the dilute magnetic semiconductor $\text{Ga}_{1-x}\text{Mn}_x\text{As}$ through hard

- X-ray angle-resolved photoemission,” *Nat. Mater.* **11**, 957–962 (2012).
9. T. Dietl, K. Sato, T. Fukushima, A. Bonanni, M. Jamet, A. Barski, S. Kuroda, M. Tanaka, H. Pham Nam, and H. Katayama-Yoshida, “Spinodal nanodecomposition in semiconductors doped with transition metals,” *Rev. Mod. Phys.* **87**, 1311–1377 (2015).
 10. A. Richardella, P. Roushan, S. Mack, B. Zhou, D. A. Huse, D. D. Awschalom, and A. Yazdani, “Visualizing critical correlations near the metal-insulator transition in $\text{Ga}_{1-x}\text{Mn}_x\text{As}$,” *Science* **327**, 665–669 (2010).
 11. L. Gluba, O. Yastrubchak, J. Z. Domagala, R. Jakiela, T. Andrearczyk, J. Zuk, T. Wosinski, J. Sadowski, and M. Sawicki, “Band structure evolution and the origin of magnetism in $(\text{Ga},\text{Mn})\text{As}$: From paramagnetic through superparamagnetic to ferromagnetic phase,” *Phys. Rev. B* **97**, No. 11, 115201 (2018).
 12. S. Zhou, “Dilute ferromagnetic semiconductors prepared by the combination of ion implantation with pulse laser melting,” *J. Phys. D: Appl. Phys.* **48**, 263001 (2015).
 13. Y. Yuan, C. Xu, R. Hübner, R. Jakiela, R. Böttger, M. Helm, M. Sawicki, T. Dietl, and S. Zhou, “Interplay between localization and magnetism in $(\text{Ga},\text{Mn})\text{As}$ and $(\text{In},\text{Mn})\text{As}$,” *Phys. Rev. Mater.* **1**, 054401 (2017).
 14. E. A. Gan’shina, L. L. Golik, V. I. Kovalev, Z. E. Kun’kova, M. P. Temiryazeva, Yu. A. Danilov, O. V. Vikhrova, B. N. Zvonkov, A. D. Rubacheva, P. N. Tcherbak, and A. N. Vinogradov, “On nature of resonant transversal Kerr effect in InMnAs and GaMnAs layers,” *Solid State Phenom.* **168–169**, 35–38 (2011).
 15. E. A. Gan’shina, L. L. Golik, Z. E. Kun’kova, V. I. Kovalev, Yu. V. Markin, A. I. Novikov, G. S. Zykov, Yu. A. Danilov, A. V. Kudrin, O. V. Vikhrova, and B. N. Zvonkov, “Magneto-optical evidence for intrinsic ferromagnetism in $(\text{Ga},\text{Mn})\text{As}$ layers grown by pulsed laser deposition,” *Solid State Phenom.* **233–234**, 101–104 (2015).
 16. E. A. Gan’shina, L. L. Golik, Z. E. Kun’kova, G. S. Zykov, I. V. Bykov, A. I. Rukovichnikov, Y. Yuan, R. Böttger, and S. Zhou., “Magneto-optical spectroscopy of diluted magnetic semiconductors GaMnAs prepared by ion implantation and further impulse laser annealing,” *J. Magn. Magn. Mater.* **459**, 141–146 (2018).
 17. Z. E. Kun’kova, E. A. Gan’shina, L. L. Golik, Yu. A. Danilov, A. V. Kudrin, V. I. Kovalev, G. S. Zykov, Yu. V. Markin, O. V. Vikhrova, and B. N. Zvonkov, “Phase separation in GaMnAs layers grown by laser pulsed deposition,” *Phys. Solid State* **60**, 943–949 (2018).
 18. B. N. Zvonkov, O. V. Vikhrova, Yu. A. Danilov, E. S. Demidov, P. B. Demina, M. V. Dorokhin, Yu. N. Drozdov, V. V. Podol’skii, and M. V. Sapozhnikov, “The use of laser sputtering for the deposition of semiconductor nanoheterostructures,” *Opt. Zh.* **75**, 56–61 (2008).
 19. D. Bürger, S. Zhou, M. Pandey, Ch. S. Viswanadham, J. Grenzer, O. Roshchupkina, W. Anwand, H. Reuther, V. Gottschalch, M. Helm, and H. Schmidt, “Application of pulsed laser annealing to ferromagnetic GaMnAs ,” *Phys. Rev. B* **81**, 115202 (2010).
 20. Y. Yuan, Y. Wang, K. Gao, M. Khalid, C. Wu, W. Zhang, F. Munnik, E. Weschke, C. Baehtz, W. Skorupa, M. Helm, and S. Zhou, “High Curie temperature and perpendicular magnetic anisotropy in homoepitaxial InMnAs films,” *J. Phys. D* **48**, 235002 (2015).
 21. E. A. Gan’shina, L. L. Golik, V. I. Kovalev, Z. E. Kun’kova, B. N. Zvonkov, and A. N. Vinogradov, “Optical and magneto-optical properties of room-temperature ferromagnetic $\text{In}(\text{Ga})\text{MnAs}$ layers, deposited by pulse laser ablation,” *J. Magn. Magn. Mater.* **321**, 829–832 (2009).
 22. P. Lautenschlager, M. Garriga, S. Logothetidis, and M. Cardona, “Interband critical points of GaAs and their temperature dependence,” *Phys. Rev. B* **35**, 9174–9189 (1987).

Translated by N. Kolchugina